

RATS-Kepler – a deep high cadence survey of the Kepler field

Gavin Ramsay¹, Adam Brooks^{1,2}, Pasi Hakala³, Thomas Barclay^{4,5},
David Garcia-Alvarez^{6,7,8}, Victoria Antoci⁹, Sandra Greiss¹⁰, Martin Still^{4,5},
Danny Steeghs¹⁰, Boris Gänsicke¹⁰, Mark Reynolds¹¹

¹ *Armagh Observatory, College Hill, Armagh, BT61 9DG, UK*

² *Mullard Space Science Laboratory, University College London, Holmbury St. Mary, Dorking, Surrey, RH5 6NT, UK*

³ *Finnish Centre for Astronomy with ESO, University of Turku, Väisäläntie 20, FI-21500 PIKKIÖ, Finland*

⁴ *NASA Ames Research Center Institute, Moffett Field, CA 94035, USA*

⁵ *Bay Area Environmental Research Institute, Inc., 560 Third St. West, Sonoma, CA 95476, USA*

⁶ *Instituto de Astrofísica de Canarias, E-38205 La Laguna, Tenerife, Spain*

⁷ *Dpto. de Astrofísica, Universidad de La Laguna, 38206 La Laguna, Tenerife, Spain*

⁸ *Grantecan CALP, 38712 Brea Baja, La Palma, Spain*

⁹ *Stellar Astrophysics Centre, Dept of Physics and Astronomy, Aarhus University, Ny Munkegade 120, DK-8000 Aarhus C, Denmark*

¹⁰ *Department of Physics, University of Warwick, Coventry, CV4 7AL, UK*

¹¹ *Department of Astronomy, University of Michigan, 500 Church Street, Ann Arbor, MI 48109, USA*

Accepted 2013 October 1. Received 2013 September 27; in original form 2013 April 2

ABSTRACT

We outline the purpose, strategy and first results of a deep, high cadence, photometric survey of the *Kepler* field using the Isaac Newton Telescope on La Palma and the MDM 1.3m Telescope on Kitt Peak. Our goal was to identify sources located in the *Kepler* field of view which are variable on a timescale of a few mins to 1 hour. The astrophysically most interesting sources would then have been candidates for observation using *Kepler* using 1 min sampling. Our survey covered $\sim 42\%$ of the *Kepler* field of view and we have obtained light curves for 7.1×10^5 objects in the range $13 < g < 20$. We have discovered more than 100 variable sources which have passed our two stage identification process. As a service to the wider community, we make our data products and cleaned CCD images available to download. We obtained *Kepler* data of 18 sources which we found to be variable using our survey and we give an overview of the currently available data here. These sources include a pulsating DA white dwarf, eleven δ Sct stars which have dominant pulsation periods in the range 24 min to 2.35 hrs, three contact binaries, and a cataclysmic variable (V363 Lyr). One of the δ Sct stars is in a contact binary.

Key words: Astronomical data bases: surveys; Physical data and processes: asteroseismology; stars: variable - white dwarf - δ Scuti

1 INTRODUCTION

The prime objective of the *Kepler* mission is to detect Earth sized planets orbiting Solar type stars in the habitable zone (Koch et al 2010). It does this by detecting transits of the host star by the orbiting exoplanet. The lightcurves which *Kepler* obtained extended over many months and have a precision of parts per million. These data allow models of stellar structure to be tested in a way that has not been possible

before (e.g. Bedding et al. 2011). Furthermore, it has led to the unexpected discovery of extreme binary systems such as the ‘*Heartbeat*’ stars which are excellent tests of binary and stellar models (Welsh et al. 2011, Thompson et al. 2012).

Asteroseismology provides the means to probe the masses and compositions of stellar interiors; determine stellar internal rotation profiles; the extent of instability strips and therefore test models of stellar structure and evolution

(e.g. Chaplin et al. 2011). To study compact objects such as pulsating white dwarfs, relatively high cadence observations are essential. For the vast majority of observations made using *Kepler*, the effective exposure time is 30 mins (*‘Long Cadence’*). However, for a much more limited number of stars (512) a shorter effective exposure of 1 min is possible (*‘Short Cadence’*).

Before the launch of *Kepler*, an extensive programme to identify bright G/K dwarfs with minimal stellar activity was carried out. Although a small number of photometric variability surveys were carried out pre-launch (e.g. Hartman et al. 2004, Pigulski et al. 2009, Feldmeier et al 2011) they were either not especially deep, did not have wide sky coverage or did not have a cadence shorter than a few minutes. To fill this gap we started a photometric variability survey (*RATS-Kepler*) in the summer of 2011 using the Wide Field Camera on the Isaac Newton Telescope (INT). Sources which were considered astrophysically interesting based on their light curve and colour would then have been the subject of bids to obtain *Kepler* Short Cadence observations.

2 PHOTOMETRIC OBSERVATIONS

Our strategy is a modified version of that used by us in the RAPid Temporal Survey (*RATS*) which was carried out using the INT between 2003 and 2010 (Ramsay & Hakala 2005, Barclay et al. 2011). In that project we obtained a series of 30 sec exposures of a given field in white light for 2.0–2.5 hrs. The resulting lightcurves had a resulting cadence of ~ 1 min and, for sources brighter than $g=21$, the standard deviation (σ) of the light curves was <0.024 mag (Barclay et al. 2011). It led to the discovery of a rare double-mode pulsating sdB star (Ramsay et al. 2006, Baran et al. 2011), pulsating white dwarfs and several dozen distant δ Sct or SX Phe stars (Ramsay et al. 2011).

Since the *Kepler* field of view (116 square degrees) is more than twice the area covered by the *RATS* project, we decided to increase the number of fields observed per night by obtaining a one hour (rather than a two hour) sequence of short exposures per pointing. Since the photometric precision of *Kepler* Short Cadence observations reduces from 12.9 percent at $g=19$ to 32.4 percent at $g=20$ (this compares with 0.85 percent at $g=16$)¹ we also reduced the exposure to 20 sec and used the g band filter instead of white light (since sources fainter than $g=20$ would give high photometric errors in *Kepler* observations).

During the summer of 2011 and 2012 we obtained data using the 2.5m INT located on the island of La Palma, and the 1.3m MDM McGraw-Hill Telescope located on Kitt Peak (see Table 1 for details). Our observations cover 42 percent of the *Kepler* field. In Figure 1 we show the position of stars observed in our survey in equatorial coordinates.

2.1 Isaac Newton Telescope

The INT Wide Field Camera has 4 CCDs and covers 0.29 degrees squared. The deadtime was 30 sec, giving a cadence of ~ 50 sec. We are sensitive to flux variations on timescales

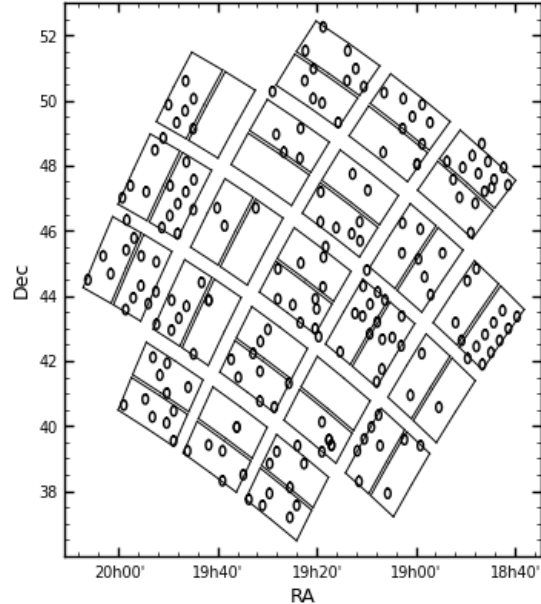


Figure 1. The field centers of our pointings which have been observed to date. Each circle has a diameter of 0.3 square degrees.

Dates	Telescope	No. Fields
11–17 Jul 2011	INT	49
01–10 Aug 2011	INT	58
16–22 May 2012	MDM	26
03–12 Aug 2012	INT	55

Table 1. The dates of observations made using the 2.5m Isaac Newton Telescope on La Palma and the 1.3m MDM Telescope on Kitt Peak. We note the number of individual fields which were subject to a 1 hr sequence of short exposures in the g band (INT) and V band (MDM).

as short as a few mins in sources with a magnitude in the range $13.5 < g < 21$. Tables A1 and A2 show the dates and field centers of each pointing.

2.2 MDM Telescope

The red4k detector was used for two nights and the MDM4k detector for five nights on the MDM Telescope². The field of view in both detectors is 0.12 degrees squared. We used a 30 sec exposure in the V band for our sequence of observations. For the red4k detector, the readout of 55 sec gave a cadence of ~ 85 sec while for the MDM4k detector the readout was 40 sec, giving a cadence of ~ 70 sec. For each field we obtained an image in BR , which were then transformed into gr magnitudes (Jester et al. 2005) with appropriate normalisation to the *Kepler* INT Survey (KIS, Greiss et al. 2012a,b) results. Table A3 shows the dates and field centers of each pointing.

¹ <http://keplergo.arc.nasa.gov/CalibrationSN.shtml>

² <http://mdm.kpno.noao.edu>

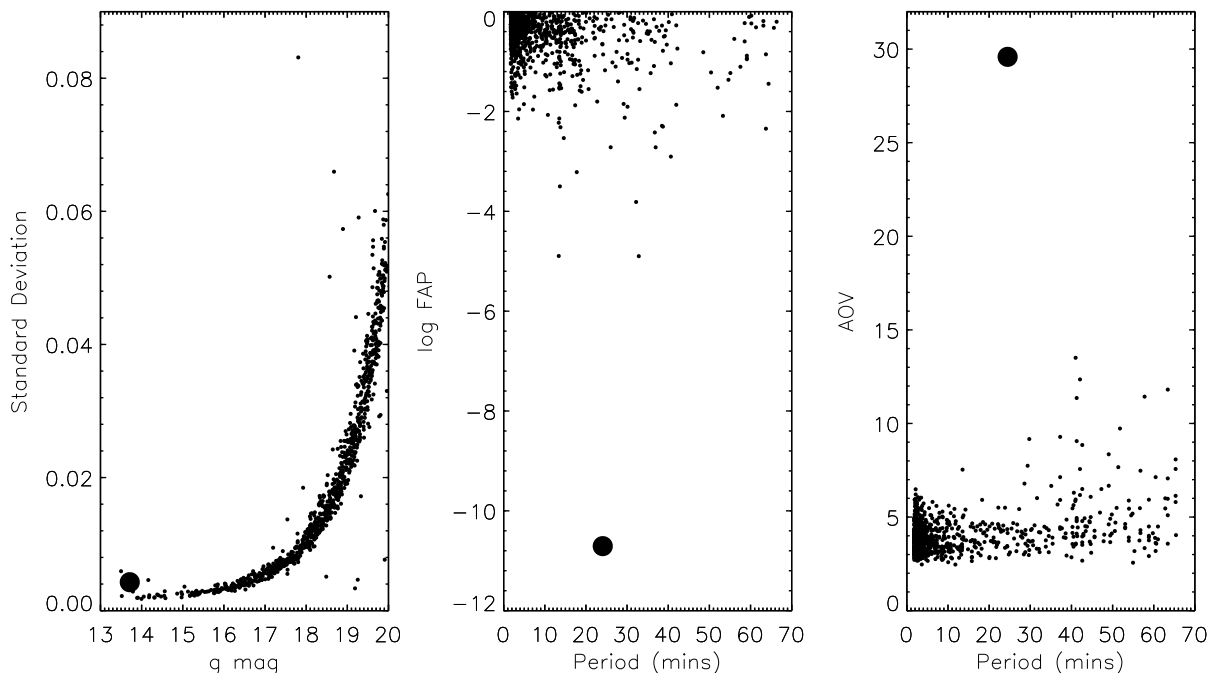


Figure 2. From left to right we plot for all stars in field 73 chip4 (which includes the short period blue variable KIC 3223460) the σ of each light curve as a function of g mag; the log FAP as a function of the period of the highest peak in the LS power spectrum; and the AOV value as a function of the AOV period.

2.3 Image Reduction

The data were corrected for the bias level and were flat-fielded using `Starlink`³ and `ftools`⁴ software. To embed sky coordinates into the images we used software made available by `astrometry.net` (Lang et al. 2010). The resulting astrometric positions agreed with the 2MASS source catalogue typically within 0.4 arcseconds. We cross-correlated the positions of our sources with that of the KIS (Greiss et al. 2012a,b) which reaches down to a limit of 20th mag in U, g, r, i and $H\alpha$ filters. We also obtained a single r band image of every INT field and a single image of every MDM field in the BR filters. We corrected our instrumental magnitudes by scaling them to agree with the KIS values using an offset derived for matched sources.

3 DATA ANALYSIS

We broadly follow the same data reduction and analysis strategy as we used for the *RATS* project, which is described in Barclay et al. (2011). However, we now outline some features specific to the *RATS-Kepler* project.

3.1 Extracting light curves

The *Kepler* field extends 6–21 degrees above the Galactic plane. Each of our individual fields are therefore relatively crowded at low latitudes or surprisingly sparse at higher latitudes. For sparse fields we used `sextractor` (Bertin &

Arnouts 1996) to extract magnitudes using aperture photometry. Differential magnitudes were determined by comparing the magnitude of each star with the mean brightness of the 3–10th most brightest stars in the image (the results were very similar if we chose, say, the 4–20th most brightest stars). For more crowded fields we used `diapl2`, an updated version of `diapl` (Wozniak 2000), which extracts photometry by applying the well established ‘Difference Imaging Subtraction’ method (Alard & Lupton 1998).

Despite the fact that differential photometry has been performed we find that the photometry of certain fields suffer from systematic trends in the data – ie the light curves derived from the same detector can show similar features. This effect can be seen in many other large scale surveys, including *Kepler* (Kinemuchi et al 2012). In our case, the systematic trends will largely result from the fact that for good technical reasons we do not use the autoguider for our INT observations. To ensure that stars remain roughly at the same position on the detector we apply manual corrections to the pointing.

However, we aimed to remove the effects of systematic trends by applying the `SYSREM` algorithm (Tamuz et al. 2005) to the light curves derived from each CCD individually using a varying number of cycles as described in Tamuz (2006) (see also Barclay et al. 2011). For a small number of fields it was not possible to detrend the data (mainly because of the low number of stars available). Using a faint limit of $g = 20.0$ and a bright limit of $g = 13.5$, we have obtained a total of 7.1×10^5 detrended light curves.

³ <http://starlink.jach.hawaii.edu/starlink>

⁴ <http://heasarc.gsfc.nasa.gov/ftools>

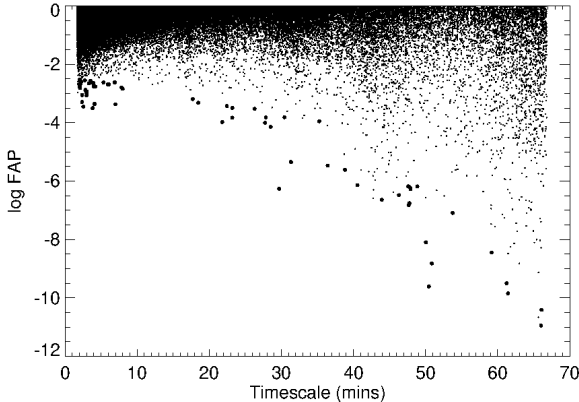


Figure 3. For those 10^5 stars located in field-chip combinations which have the least negative median log FAP, we plot the log of the False Alarm Probability (FAP) as a function of the period of the most prominent peak in the Lomb Scargle power spectrum. More negative values of log FAP imply a greater chance of intrinsic variability. Those sources which have been identified as variable candidates using the MAD statistic with $n=14$ are shown as larger filled circles (see §3.2 for details).

3.2 Identifying variable candidates

Identifying *bona fide* variable stars from a large sample of light curves is not a trivial task. Here we use a two stage process of identifying variable stars. In the first stage we use different statistical tests to obtain a sample of candidate variables. In the second stage we manually perform a quality assessment of each light curve and associated images to remove sources which have been spuriously identified as variable.

Different statistical tests are better suited to identifying different kinds of variability. For instance, the Lomb Scargle (LS) Periodogram (Lomb 1976, Scargle 1982) is particularly well suited to detecting pulsating variables where the pulsation period is shorter than the duration of the light curve. On the other hand, the Alarm test (Tamuz, Mazeh & North 2006) and the Analysis of Variance (AoV) test (Schwarzenberg-Czerny 1989, 1996 and Devor 2005 for the implementation used by VARTOOLS) are suitable for identifying eclipsing or contact binaries, whilst the χ^2 test (where the model is the mean magnitude of the light curve) is good for detecting flare stars (see Graham et al. 2013 for a recent review of which tests are best suited to identifying specific kinds of variable star).

The VARTOOLS suite of software (Hartman et al. 2008) allows the parameterisation of large numbers of light curves using many different statistical tests in a quick and simple manner. We apply the following tests on each of our light curves: the LS Periodogram; the Alarm test and the AoV test. We also determine the χ^2 value and standard deviation (σ) for each light curve after applying a 5σ clipping to each light curve. A file containing the positions and colours of all sources along with their photometric variability parameters can be downloaded via Armagh Observatory Web

Site (star.arm.ac.uk/rats-kepler). Table A4 outlines the full set of parameters which are given in this FITS file.

As an example of how different tests compare, we show in Figure 2 the results of the σ , LS and AoV tests on a field which contains KIC 3223460 which has a dominant pulsation period of 24.2 mins (see Table 2). Plotting the σ of each light curve as a function of g mag shows that KIC 3223460 has a greater σ than the main distribution of sources with similar magnitude. However, there is (naturally) no information on the timescale of variability. On the other hand, the LS and AoV test clearly identify KIC 3223460 as being strongly variable on a period of 24 mins.

The main goal of our survey is to identify compact pulsating stars in the *Kepler* field which would then have been the subject of bids to observe them in Short Cadence mode using *Kepler*. As demonstrated in Figure 2, the LS Periodogram is efficient at identifying these sources in our data. The LS Periodogram as implemented in VARTOOLS determines the frequency of the highest peak in the power spectrum (which we define as the ‘Period’ of variability even if the source cannot be verified as strictly periodic) and the False Alarm Probability of this peak being statistically significant. For each light curve we obtained an LS power spectrum and performed the AoV test in the frequency interval corresponding to the Nyquist frequency (847.1 cycles/day – which equates to a period of 1.7 mins – for the INT data and 600 cycles/day – which equates to a period of 2.4 mins – for the MDM data) and 21.49 cycles/day – which equates to a period of 67 mins – (which is the mean duration of the INT light curves).

For the purposes of selecting an initial sample of candidate variables, we use the LS test. In the absence of red noise and systematic trends, a peak in the power spectrum with log FAP = -2.5 is likely to be significantly variable at the 3σ confidence level. However, since the seeing and sky brightness can vary from field to field, and the success of the detrending algorithm can vary from chip to chip, the threshold for identifying variables can be more negative than log FAP = -2.5 .

We determined the median value of the log FAP statistic for the light curves in each field-chip combination. We then ordered our sources by this median log FAP and made seven sub-sets containing 10^5 stars each (the remaining 8787 stars which were in field-chip combinations with the highest median log FAP were discarded). For the subset with the least negative mean value for log FAP (Figure 3), there were 911 sources which has a log FAP < -2.5 (or 0.91 percent of sources in the sub-set).

Rather than using a fixed threshold for the log FAP to provide an initial selection of candidate variables, we used the Median Absolute Deviation (MAD) to provide a means of identifying sources which were ‘outliers’ in the Period - log FAP distribution. The MAD is defined for a batch of parameters $\{x_1, \dots, x_m\}$ as

$$\text{MAD} = \text{median}_i(|X_i - \text{median}_j(X_j)|) \quad (1)$$

We ordered the data by Period and then into 2 min time bin intervals and derived the MAD for each bin. Candidate variables are then selected so that variable sources obey $(\log \text{FAP}) < \text{MAD}_{\log \text{FAP}} \times n + \text{Median}_{\log \text{FAP}}$, where n is an integer which defines how far a source is from the local median log FAP. It is selected largely by trial and er-

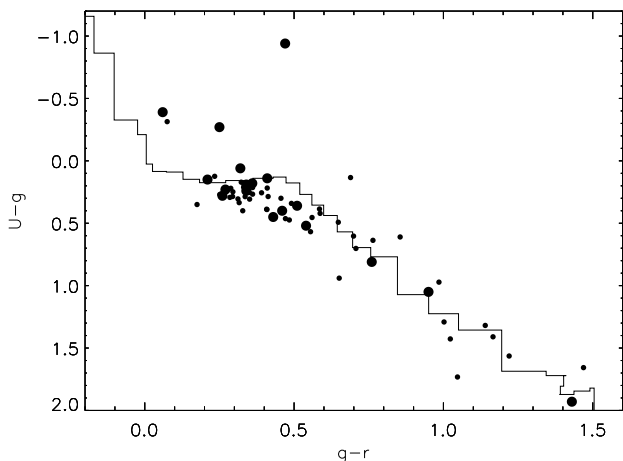


Figure 4. The solid line shows the unreddened main sequence (taken from Groot et al. 2009). Small circles indicate the colours of sources shown in Table A5 while larger circles indicate the colours of those sources which we have obtained *Kepler* Short Cadence data (Table 2).

ror – too high a value of n will select only the most strongly variable sources, but too low a value of n will produce large quantities of candidate variables, all of which require manual verification. (To be selected as a candidate variable, a source also has to have $\log \text{FAP} < -2.5$). The selection of variables using the MAD statistic was done on each subset of 10^5 stars separately then combined according to the n value that was used. We found that for $n=18$, 227 stars (or 0.032 percent of the total) were selected as candidate variables ($n=16 \rightarrow 368$ stars, $n=14 \rightarrow 642$, $n=12 \rightarrow 1187$, $n=10 \rightarrow 1999$). We stress that this selection simply identifies those stars which are most likely to be variable.

Each source is then subject to a manual inspection of the light curve and corresponding images to verify their variable nature. Where appropriate, additional light curves were obtained using the optimal aperture photometry routine *autophotom* (Eaton, Draper & Allan 2009). In this process we assign a Flag value (see Table A4) to characterise their lightcurve and timescale of variability. For our $n=18$ sample we found that after a second stage verification process we had 65 sources which we classed as highly likely to be variable using the LS statistic as a first screening stage. A summary of these sources are shown in Table A5 and their colours are shown in Figure 4. By examining samples derived using $n=14$, we have found more than 100 sources which have passed our two stage variable identification process. These are indicated in the FITS file which we make available on the Armagh Observatory Web site.

A high fraction of sources (71 percent) of the $n=18$ sample were found to be unlikely to be *bona fide* variable sources. Many of these spurious variables were caused by residual systematic trends in the light curves - for instance sources from the same chip showed very similar trends in their light curves. This is almost certainly a result of using manual corrections in the guiding process in the INT observations and for the fact that the light curves only covered a short time (typically 1 hr).

We selected 18 sources which would be good targets to observe using *Kepler* in 1 min sampling mode. We suc-

cessfully bid for *Kepler* Guest Observer Programme and the Directors Discretionary Time Programme. We show the INT light curves of these sources in Figure 5 and we give their sky coordinates, magnitude, colours in Table 2. We indicate an approximate spectral classification using our INT and Gran Telescopio Canarias (GTC) spectra (§4). Of these 18 sources, one is a pulsating DA white dwarf (the details are presented in Greiss et al in prep), three are contact binaries, one is a cataclysmic variable, and one is a flare star (Ramsay et al. 2013). However, most of these sources appear to be δ Sct stars. We will present an overview of the *Kepler* data of these sources in §5.

4 OPTICAL SPECTROSCOPY

As part of our follow up programme, we obtained low-medium resolution optical spectroscopy of over 50 sources which were either identified as being variable on a short timescale or had unusual colours. (One very blue source in our sample, KIC 10449976, has already been reported as an extreme helium star, Jeffery et al. 2013). We obtained data using the Intermediate Dispersion Spectrograph (IDS) and the R400 grism on the INT between 26–28 June 2012 and also using the Optical System for Imaging and Low Resolution Integrated Spectroscopy (OSIRIS) tunable imager and spectrograph and the R1000R grism on the 10.4 m GTC during March – June 2013. Both are located at the Observatorio Roque de los Muchachos in La Palma, Canary Islands, Spain. At least two spectra were obtained of each source and the individual exposure time ranged from 180 to 360 sec (INT) and 40 to 400 sec (GTC). The spectra were reduced using standard procedures with the wavelength calibration being made using a CuNe+CuAr arc taken shortly after the object spectrum was taken. A flux standard was observed so that the (resulting combined) spectra of each source could be flux calibrated in the case of the IDS spectra and to remove the instrumental response in the OSIRIS spectra (the observing programme utilises poor observing conditions). The spectral resolution of our INT spectra was $\sim 2\text{\AA}$ and $\sim 8\text{\AA}$ for our GTC spectra.

For stars which were of the spectral type A/F we modelled the spectra using a grid of LTE models calculated using the ATLAS9 code (Kurucz 1992) with convective overshooting switched off. Spectra were calculated with the LINFOR line-formation code (Lemke 1991). Data for atomic and molecular transitions were compiled from the Kurucz line list. The stellar temperatures were estimated from the hydrogen Balmer lines of the stars ($H\beta$ to $H\delta$) using the FITSB2 routine (Napiwotzki et al. 2004). No gravity sensitive features are accessible in our low resolution spectra. McNamara (1997) finds that SX Phe and large amplitude δ Sct stars have a range in $\log g$ of 3.0–4.3. In our fits we fixed $\log g=4.0$, although the resulting temperature is only weakly sensitive to this parameter. The metallicity was allowed to vary although this was not strongly constrained in the fits. The error of the fit parameters were determined with a bootstrapping method. As an example of the fits we show in Figure 6 the fit to the spectrum of KIC 3223460. We show in Table 3 the temperature we derive for the stars which we have obtained *Kepler* Short Cadence data (§5). We make all the spectra available through the the Armagh Observatory

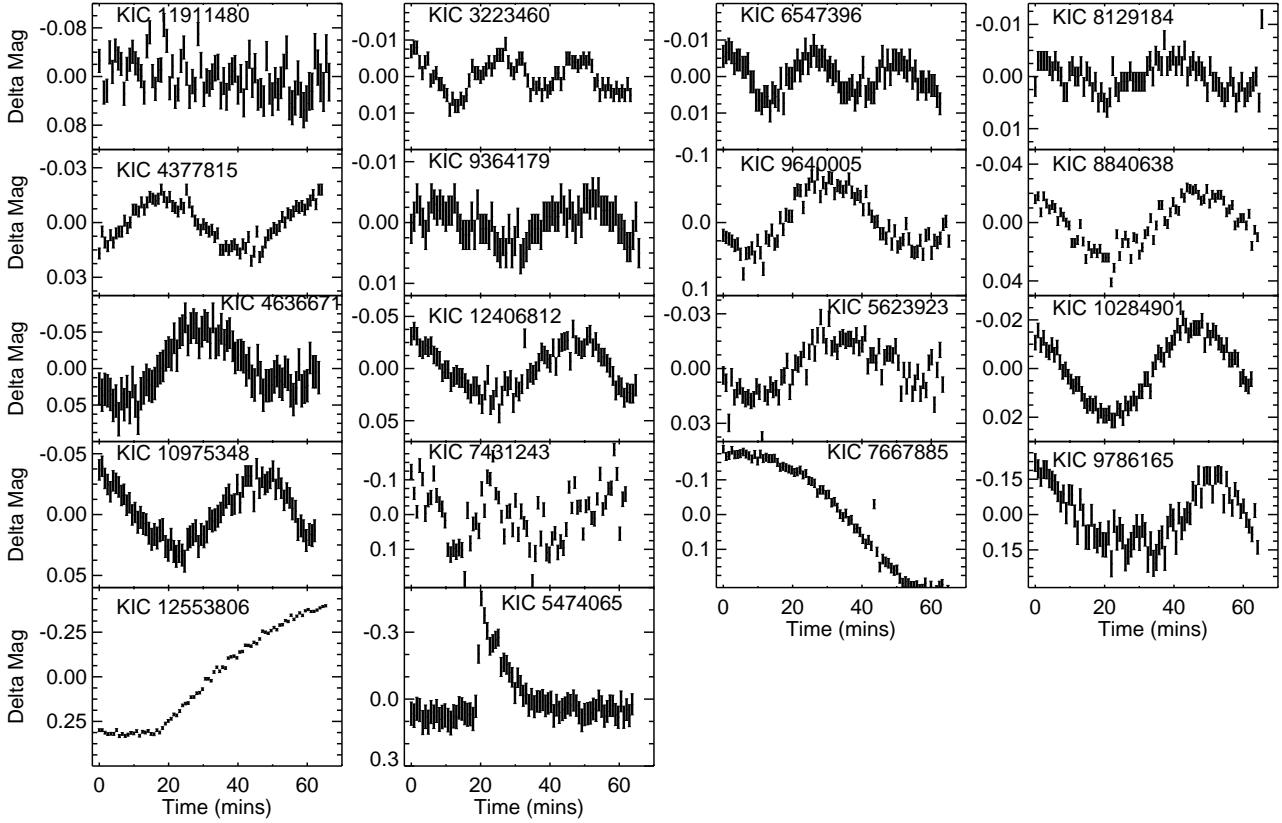


Figure 5. The INT light curve of those sources which have been identified as variable in the *Kepler*-RATS survey and which we have obtained *Kepler* Short Cadence data. The details of these sources are shown in Table 2.

KIC	RA (J2000)	DEC (J2000)	g	$U-g$	$g-r$	<i>Kepler</i> SC Data	Period Kepler	Spectra	Spectral Type	Variable Type
11911480	19 20 24.9	+50 17 22.4	18.13	-0.39	0.06	12,16	290 sec			DAV (1)
3223460	19 12 32.2	+38 23 00.1	13.74	-0.27	0.25	14	24.2 min	GTC	mid-late A	δ Sct
6547396	19 53 18.3	+41 58 26.9	14.84	0.40	0.46	16	26.6 min	INT	mid-late A	δ Sct
8120184	19 54 11.9	+43 59 20.1	14.27	0.36	0.51	15	42.6 min	INT	mid-late A	δ Sct
4377815	19 39 08.1	+39 27 35.9	14.83	0.24	0.34	15	45.7 min	INT	mid-late A	δ Sct
9364179	19 56 24.5	+45 48 24.1	14.38	0.45	0.43	15	46.8 min	INT	mid-late A	δ Sct
9640005	19 09 46.3	+46 20 04.1	18.40	0.15	0.21	14–16	49.5 min	GTC	mid A	δ Sct
8840638	19 55 35.1	+45 04 46.0	14.63	0.52	0.54	14–16	49.6 min	GTC	mid-late A	δ Sct
4636671	19 01 52.2	+39 45 59.3	15.67	0.28	0.26	14–16	50.0 min	GTC	mid A	δ Sct
12406812	19 23 33.8	+51 17 58.9	17.24	0.18	0.36	14–16	50.4 min	GTC	mid-late A	δ Sct
5623923	19 32 01.5	+40 51 16.8	16.62	0.23	0.27	14–16	50.5 min	GTC	mid-late A	EB+ δ Scuti
10284901	19 43 46.4	+47 20 32.8	15.73	0.06	0.32	14,16	75.8 min	GTC	mid-late A	δ Sct
10975348	19 26 46.1	+48 25 30.8	18.89	0.19	0.34	14–16	2.35 hrs	GTC	mid A	δ Sct
7431243	19 08 51.6	+43 00 31.5	19.10	-0.94	0.47	16	4.68 hrs			CV (2)
7667885	19 03 30.2	+43 23 22.7	17.64	1.05	0.95	14–16	7.56 hrs	GTC	mid G	W UMa
9786165	19 50 11.0	+46 34 40.8	17.67	0.81	0.76	14,16	7.98 hrs	GTC	mid G	W UMa
12553806	19 14 41.0	+51 31 08.9	17.52	0.14	0.41	14–16	11.12 hrs	GTC	A+F?	W UMa
5474065	19 53 02.5	+40 40 34.6	18.77	1.93	1.43	14	Flare	GTC	M3 V	Flare star (3)

Table 2. The details of those sources whose light curve is shown in Figure 5. We indicate their KIC ID; their RA and Dec; the g mag, $(U - g)$ and $(g - r)$ colours, which have been taken from the KIS (Greiss et al. 2012a,b). We also show in which Quarter *Kepler* Short Cadence (SC) data was obtained and what the dominant period was in the power spectrum of the *Kepler* light curve. In the ‘Spectra’ column we indicate if we obtained a spectrum of the source using the INT or GTC, what the approximate spectral type was and in the last column what the type of variable star the source is. EB: Eclipsing Binary. Notes: (1) Greiss et al. in prep, (2) Cataclysmic Variable, Scaringi et al. 2013), (3) Ramsay et al. (2013).

KIC	T_{GTC}	T_{IDS}	T_{KIC}	$\log g_{KIC}$
3223460	8180±110		7930	4.1
6547396		8290±110	7480	4.0
8120184		7760±180	7290	3.7
4377815		7880±160	7740	4.0
9364179		7860±180	7000	4.0
9640005	7730±180			
8840638	7860±120		6310	3.8
4636671	7950±120		7640	4.0
12406812	7660±140		7370	4.1
5623923	7970±110		8300	3.9
10284901	7710±180		8420	4.0

Table 3. For those sources which we have observed using *Kepler* we show the temperature we derive from INT and GTC spectra along with the temperature and log g taken from the *Kepler* Input Catalog (Brown et al. 2011). The errors for T_{GTC} and T_{INT} refer to the formal 3σ confidence interval. Including systematic uncertainties, which have not been included, we estimate the realistic 3σ uncertainties are ± 300 K. The uncertainties for T_{KIC} and $\log g_{KIC}$ are ± 250 K and ± 0.25 dex respectively (c.f. Brown et al. (2011) and Pinsonneault et al. (2012)).

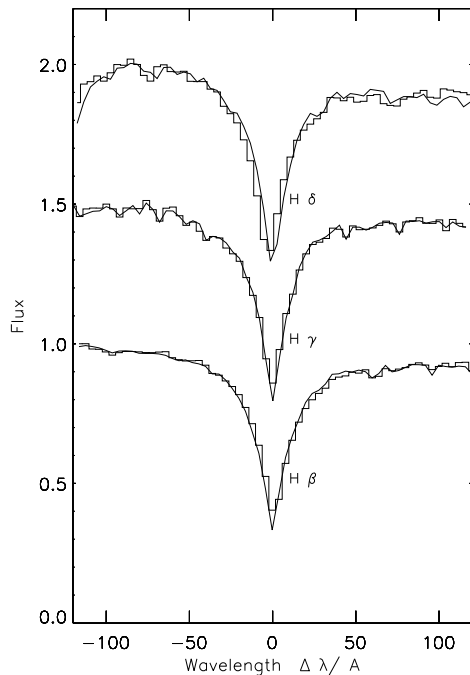


Figure 6. As an example of the spectral fits to our optical spectra, we show the fit to KIC 3223460. For each spectral line, the continuum has been normalised to unity and each spectrum after H_{β} has been shifted up by 0.5 flux units.

Web site (<http://star.arm.ac.uk/rats-kepler>) together with the fitted temperature of each.

5 Kepler OBSERVATIONS

The detector on board *Kepler* is a shutterless photometer using 6 sec integrations and a 0.5 sec readout. There are two modes of observation: *long cadence* (LC), where 270 in-

tegrations are summed for an effective 28.4 min exposure, and *short cadence* (SC), where 9 integrations are summed for an effective 58.8 sec exposure. When an object is observed in SC mode, LC data is also automatically recorded. After the data are corrected for bias, shutterless readout smear and sky background, light curves are extracted using simple aperture photometry (SAP). Data which were contaminated, for instance during intervals of enhanced solar activity, were removed by requiring data to be flagged by the FITS keyword ‘SAP_QUALITY’=0, and the data were corrected for systematic trends (Kinemuchi et al. 2012).

The *Kepler* data on the pulsating DA white dwarf will be presented in full by Greiss et al. (in prep) while the *Kepler* data on the flare star KIC 5474065 has been presented by Ramsay et al. (2013). Here we give a brief overview of the *Kepler* data on the pulsating, contact binaries and cataclysmic variable which we have obtained.

5.1 δ Sct stars

In Table 2 we identify eleven sources which show a dominant period in the range 24.2 min to 2.35 hrs. Our fits to their low resolution spectra (Table 3) indicate that they have a temperature in the range ~ 7600 – 8300 K. They are therefore consistent with the characteristics of δ Sct and SX Phe stars (see Breger 2000 for a review). We show a short section (1 day) of each of the *Kepler* light curves of these δ Sct type stars in Figure 7. Using a full month of data, we find that their power spectra are complex and show many frequencies (Figure 8).

The δ Sct stars with the shortest pulsation periods in our sample are KIC 3223460 (24 min) and KIC 6547396 (26 min). Indeed, they are at the extreme short period end of the δ Sct star distribution (18 mins marks the short period end, Uytterhoeven et al. 2011). The discovery of two δ Sct stars with such a short period will therefore provide an opportunity to discover the internal structure of these sources through asteroseismology. Eight of our sample, (KIC 8120184, 4377815, 9364179, 9640005, 8840638, 4636671 and 5623923), have a peak in their power spectra which lies in the range 42.6 – 50.5 mins. They have a best fit temperature in the range 7660–7950 K (Table 3). The longest period pulsators, KIC 10284901 (75.8 mins) and 10975348 (2.35 hrs) also show high amplitude variations and appear to be high amplitude δ scuti stars which occupy a restricted range of the instability strip (McNamara 2000).

Decades of research have shown that the light curves of δ Sct stars are very complex (e.g. Pamyatnykh 2000, Breger 2000). However, this makes them very useful astrophysical laboratories as they show physical phenomena which can be used to test theoretical models. However, in many δ Sct stars it is difficult to uniquely identify modes in the power spectra of the light curve. An exception is slow rotators such as 44 Tau (Lenz et al. 2010) where a large variety of pressure and gravity modes were identified. For the majority of these stars, when it comes to modelling their power spectra, a major difficulty is that the mechanism selecting which modes are excited to observable amplitudes is not well understood (Dziembowski & Krolikowska 1990). In other words, some modes are excited while others are not, which makes identifying the specific mode for each peak in the frequency spectra difficult.

The δ Sct stars are stars with masses between 1.5 and $2.5 M_{\odot}$ and their pulsations are thought to be driven largely by the opacity mechanism in the HeII ionisation zone (Baker & Kippenhahn 1962). From *Kepler* and *CoRoT* observations, however, it seems that the opacity mechanism alone cannot excite the entire range of observed modes. This means that either the models are incomplete or that there is an additional mechanism contributing to the driving. Such an alternative explanation would be the presence of stochastically excited modes, like in the Sun. Theoretical models in fact predict the convective envelopes of δ Sct stars are still deep and effective enough to drive Solar-like oscillations. Recently, Antoci et al. (2011), suggested the detection of such a hybrid star, showing κ mechanism and stochastically driven modes. However longer observations revealed that the interpretation is more complicated than initially anticipated (Antoci et al. 2013). It is therefore of great importance to find pulsating stars with similar temperature and gravity to HD 187547 ($T_{eff}=7500\pm 250$ K, $\log g = 3.9\pm 0.25$, Antoci et al. 2011) to test current models. Many of our δ Sct stars have a similar temperature to HD 187547 but spectra with higher spectral resolution than the ones we present in §4 are required to provide a robust temperature determination. However, even if our δ Sct stars are likely to be too faint to identify their pulsation modes (even the brightest of our sources at $g=13.7$ is relatively faint for such an analysis), the frequency range and the stability of excited modes can lead to a better understanding of the pulsation mechanisms, provided the temperature is robustly determined.

5.2 Contact Binaries

The *Kepler* data of three of the sources shown in Table 2 and Figure 5 clearly indicate that they are eclipsing or contact binaries with an orbital period ranging from 0.315 days – 0.463 days. We show the *Kepler* Q14 SC data of these sources in Figure 9 where we have folded and binned the data on the orbital period.

Prša et al. (2011) and Slawson et al. (2011) present an analysis of the first and second *Kepler* data release of 4044 eclipsing and contact binaries. Although the shape of the folded light curves of KIC 7667885 and KIC 12553806 are similar to that of semi-detached binaries (also known as β Lyr binaries), their relatively short orbital period suggests that they are more likely to be contact binaries (also known as W UMa binaries). The folded light curve of KIC 9786165 also implies it is a contact binary. Although some caution has to be applied in interpreting the results of our spectral fits since we have applied a single temperature model to sources which are clearly binary systems, the temperatures which we derive (Table 3) indicate they are contact binaries rather than semi-detached binaries which have B star components (and hence much hotter).

Unlike the three sources outlined here which have been observed using SC mode, none of the sources shown in Prša et al. (2011) or Slawson et al. (2011) have been observed in SC Mode. Since each of the three binaries have a high inclination, they are excellent data-sets to search for third bodies (such as exo-planets) in these systems.

5.3 KIC 5623923: A δ Sct star in a contact Binary

We show a 2.5 day section of the light curve of KIC 5623923 in Figure 10. It is clear that this source is an eclipsing or contact binary system with a orbital period of 1.21 days. However, there are clear pulsations on a period of ~ 50 mins superimposed on the light curve. The pulsations are not readily apparent during the secondary eclipses indicating that the secondary star (the less luminous of the binary components) is the source of the pulsations.

There are at least two other eclipsing or contact binary stars in the *Kepler* field which have a δ Sct component. KIC 4544587 is a binary system with a 2.18 day orbital period (Hambleton et al. 2013) while KIC 10661783 has an orbital period of 1.23 days (Southworth et al 2011). Unlike KIC 5623923 where the secondary star is the pulsating component, in both KIC 4544587 and KIC 10661783 the primary is the pulsating star. We note that the spectral fits suggest a temperature of 8000 K (Table 3) although we have fitted only a single temperature to a system which is clearly a binary.

The power spectrum of KIC 5623923 (Figure 11) shows many peaks in the 20-30 cycles/day frequency interval which are due to pressure (p) mode pulsations in the secondary star. Some of these peaks are separated by 0.83 cycles/day which is the orbital period. This implies that the amplitude of the δ Sct pulsations are correlated with the orbital period (see Shibahashi & Kurtz 2012 for a discussion on how power spectra can be used to measure radial velocities in binary systems). The power spectrum of KIC 10661783 shows peaks in its power spectrum in a similar frequency range (Southworth et al. 2011) while the p-modes seen in KIC 4544587 (Hambleton et al. 2013) are at a higher frequency range (40-50 cycles/day). We defer a full analysis of these *Kepler* data for a dedicated paper.

5.4 KIC 7431243 (V363 Lyr): A Cataclysmic Variable

KIC 7431243 was found to be a moderately blue source in the KIS ($g - r=0.47$, Greiss et al. 2012) and in our survey it was found to show rapid flux changes superimposed upon an irregular variation (Figure 5). KIC 7431243 matches the variable star V363 Lyr which was discovered as a Cataclysmic Variable (CV) by Hoffmeister (1967), whilst Kato et al (2001) found that it shows outbursts of duration 7–8 days every ~ 21 days. There are several dozen known CVs in the *Kepler* field (see Scaringi et al. 2013 and Howell et al. 2013).

KIC 7431243 was observed using *Kepler* in Q16 for 5.2 days and (not surprisingly) no outbursts were seen (Figure 12). The power spectrum of the light curve shows peaks corresponding to 4.68 hrs and 4.47 hrs. If we attribute the longer period to the super-hump period (super-humps are caused by the precession of the accretion disk) and the shorter period to the orbital period, we find the fractional excess, $\epsilon^+ = (P_{sh} - P_{orb})/P_{orb}=4.7$ percent. Using the relationship of Patterson et al. (2005) this would imply a mass ratio, $q = M_2/M_1 \sim 0.21$.

Using the secondary star mass (M_2) – orbital period relationship for CVs ($M_2 = 0.065P_{hrs}^{5/4}$, Warner 1995), we find for a CV with $P_{orb}=4.47$ hrs, $M_2=0.42M_{\odot}$ ($0.45M_{\odot}$ for

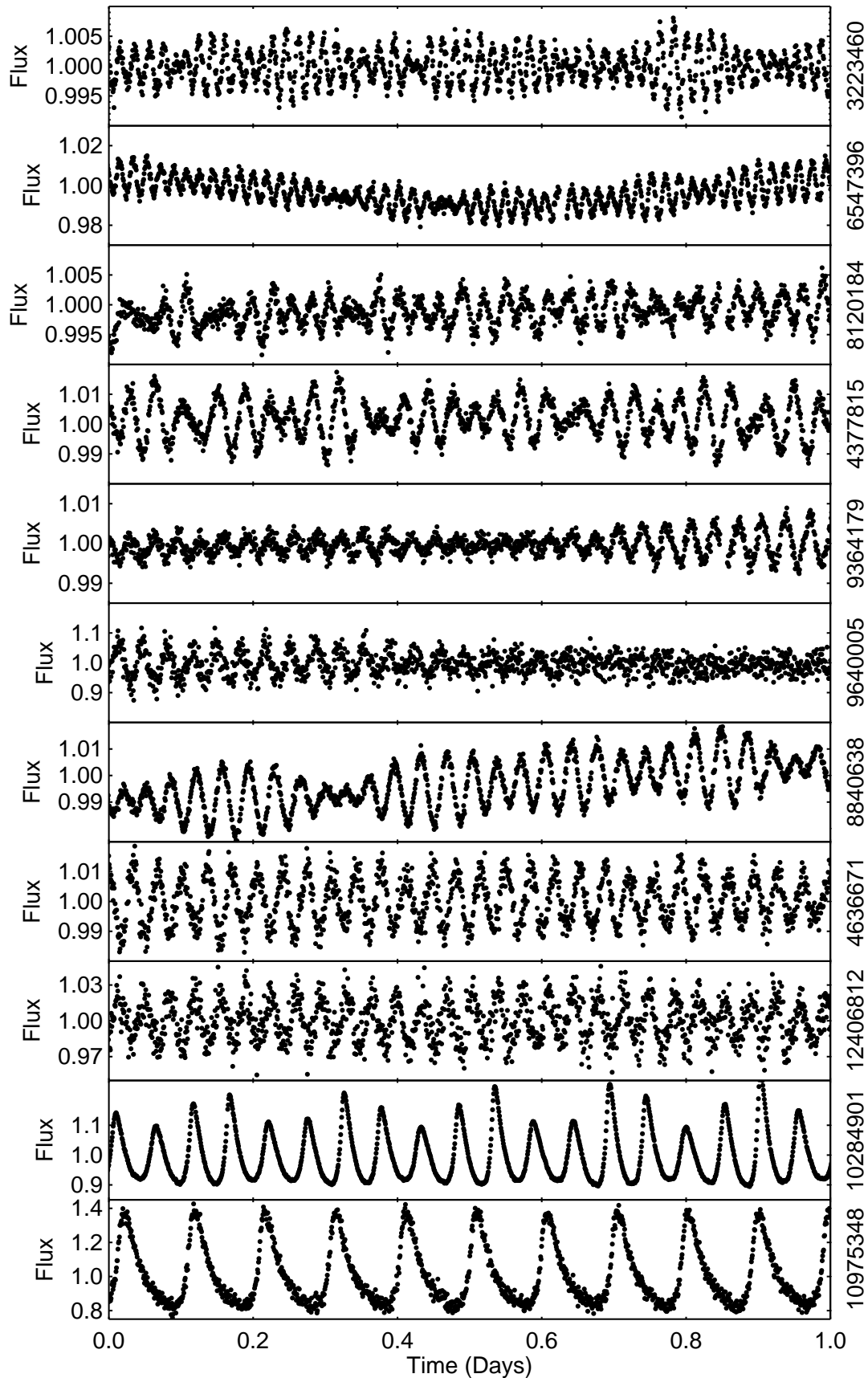


Figure 7. The *Kepler* SC light curves of the eleven sources which appear to be δ Sct type stars. They are ordered so that those showing the shortest dominant period is at the top of the figure. For clarity we show the light curve covering only one day for each star. The KIC identifier for each star is shown on the right hand edge of each panel.

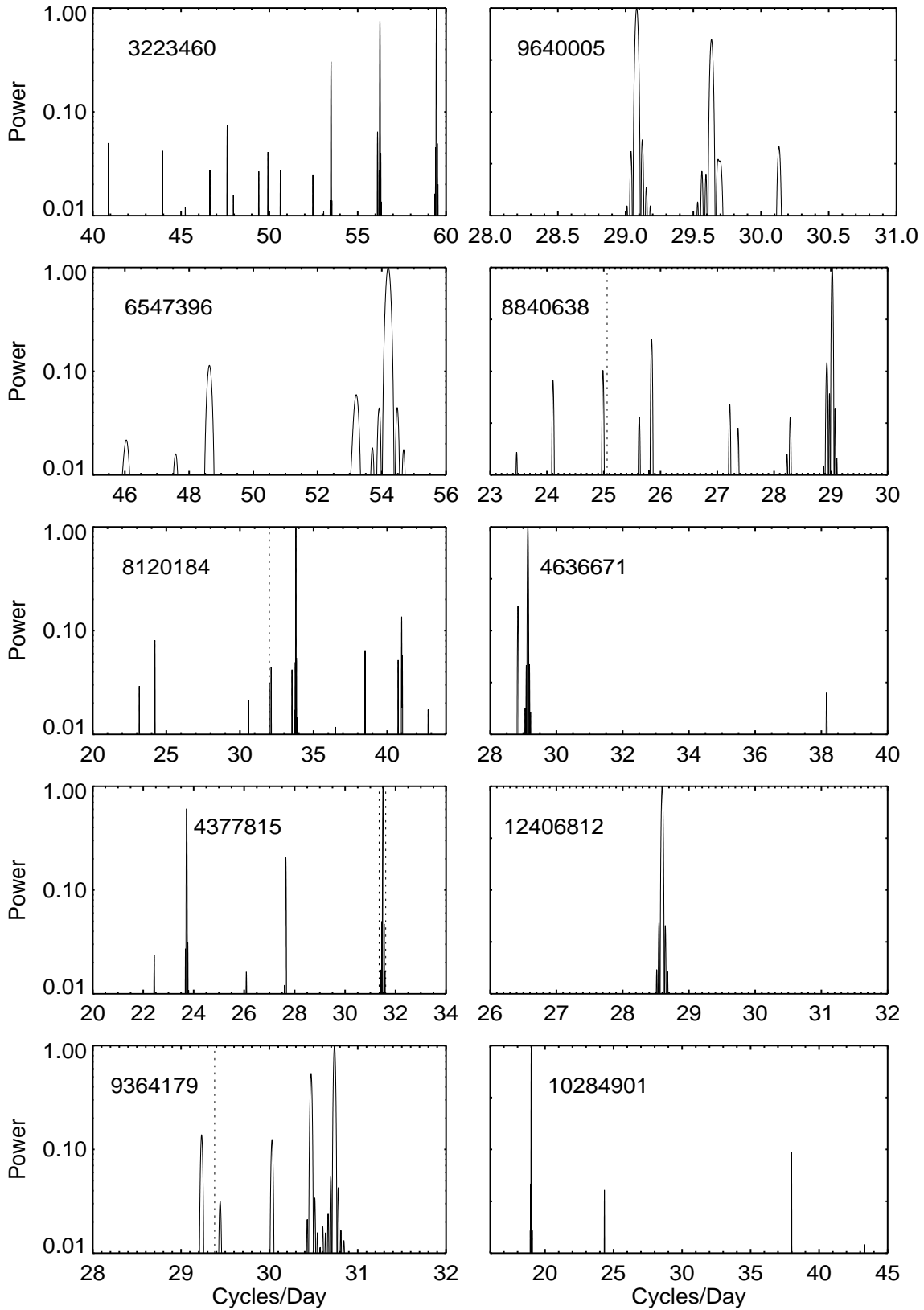


Figure 8. The power spectra of ten of the sources shown in Figure 7 (we omit for reasons of space the longest period system shown in Figure 7). We have normalised the power spectra so that maximum power is unity, plot the power in log space, and we focus on the frequency range of interest in each star. The KIC identifier for each star is shown in each panel. The light curves for each star shown here cover one month of data except for KIC 6547396 the data was taken in quarter 16 and covers 5.2 days. Dashed vertical lines indicate known artifacts in the power spectra of *Kepler* SC data.

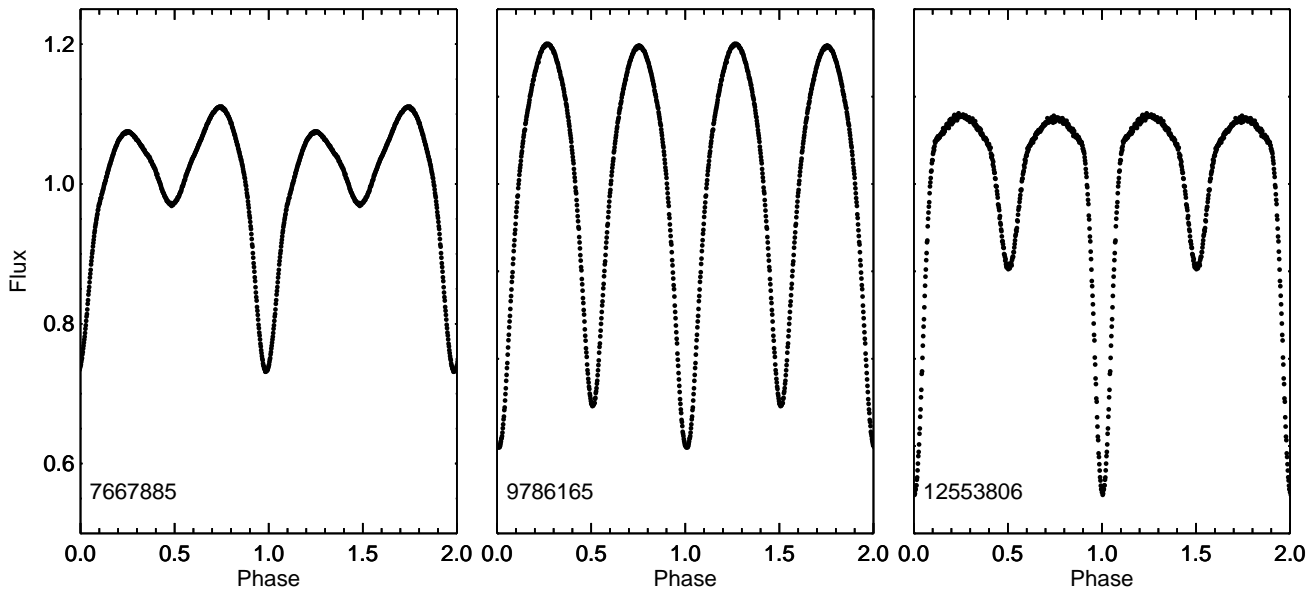


Figure 9. The *Kepler* light curve of the contact binaries KIC 7667885, KIC 9786165 and KIC 12553806. The data have been phased so that the primary eclipse is centered on $\phi=0.0$ and the y-axis is plotted on the same scale in each panel.

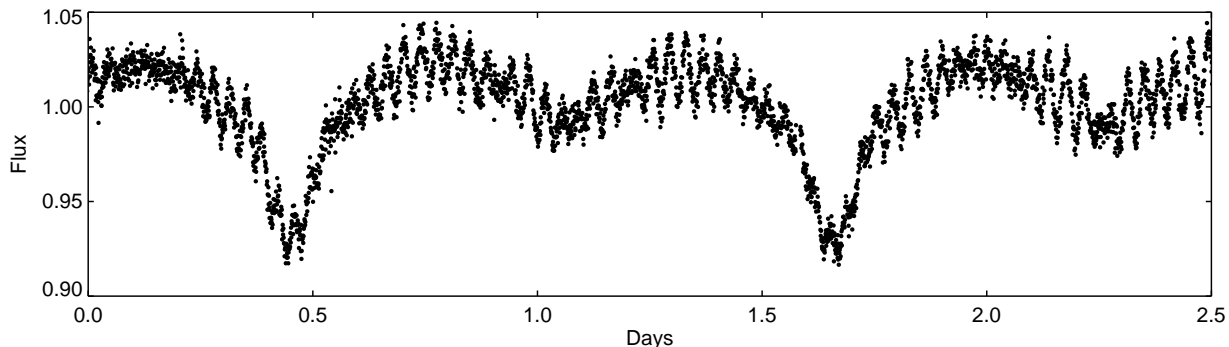


Figure 10. A short section of Q14 *Kepler* data of KIC 5623923. The binary component which is obscured during the secondary eclipse shows clear evidence of pulsations.

$P_{orb}=4.68$ hrs). Super-humps are thought to be restricted to systems where the mass ratio, $q = M_2/M_1 < 0.33$, (see Schreiber 2007 for details). If super-humps are present in KIC 7431243 then this may suggest that the white dwarf in this binary has a mass $M_1 > 1.28 M_\odot$ assuming $M_2=0.42M_\odot$ ($M_1 > 1.36 M_\odot$ for $M_2=0.45M_\odot$). Given the potentially high mass of the white dwarf, we urge phase resolved optical spectroscopy this system.

6 CONCLUSIONS

This project set out to identify sources in the *Kepler* field which showed variability on a timescale of 1 hour or less. The most potentially interesting of these variable sources would then have been subject of bids to obtain *Kepler* data in Short Cadence. We have identified more than 100 strongly variable sources and we have been successful in obtaining *Kepler* SC light curves of 18 of these sources.

Many of them are δ Scuti stars which show an astonishing range of variability, the star with the shortest dominant

period being 24 min. We also identify one δ Scuti star as being in an eclipsing or contact binary with an orbital period of 1.21 days. As currently only two other such systems are known in the *Kepler* field, this will provide the means to study binary evolution in more detail. We have also obtained *Kepler* SC data of three contact binaries and one previously known Cataclysmic Variable. The *Kepler* observations of one flare star and one pulsating DA white dwarf are reported elsewhere.

We provide a range of images and data products through the Armagh Observatory Web Site (star.arm.ac.uk/rats-kepler). These include the reduced images so that users can perform photometric measurements using their favoured reduction packages. We also provide the detrended light curves and the photometric variability parameters of each source observed in our survey.

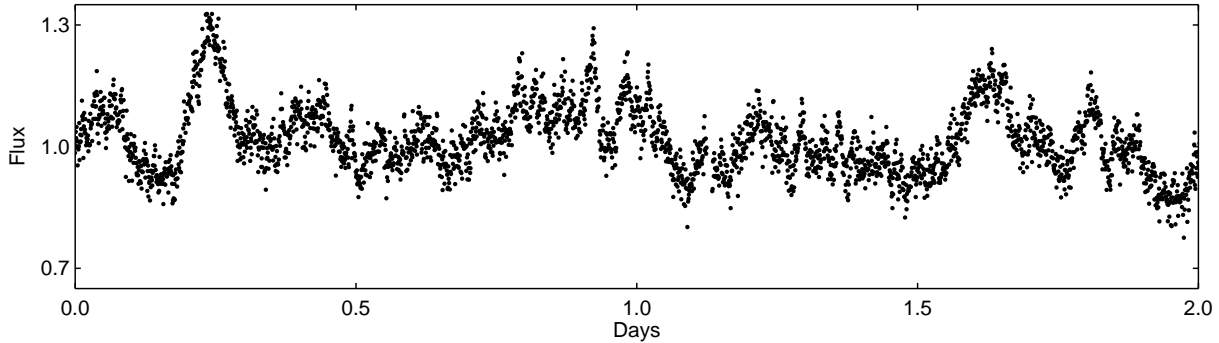


Figure 12. The *Kepler* short cadence light curve of KIC 7431243 (V363 Lyr) shown over a 2 day time interval.

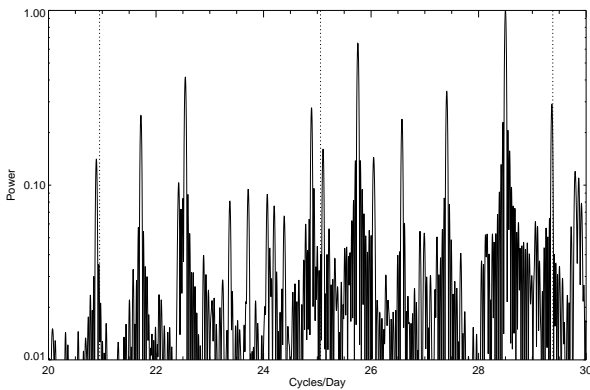


Figure 11. The power spectrum of the Q14 *Kepler* light curve of KIC 5623823. The spacing between some peaks correspond to the orbital frequency suggesting that the amplitude of the δ Sct pulsations are correlated with the orbital period. Dashed vertical lines indicate known artifacts in the power spectra of *Kepler* SC data.

7 ACKNOWLEDGEMENTS

The Isaac Newton Telescope is operated on the island of La Palma in the Spanish Observatorio del Roque de los Muchachos of the Instituto de Astrofísica de Canarias (IAC) with financial support from the UK Science and Technology Facilities Council. We would like to thank the ING and MDM staff for their support. Observations were also made with the Gran Telescopio Canarias (GTC) which is also sited on La Palma and run by the IAC. Armagh Observatory is supported by the Northern Ireland Government through the Department of Culture, Arts and Leisure. We thank Wojtek Pych for the use of his difference imaging software *diap12*. DS acknowledges support of STFC through an Advanced Fellowship. Funding for the Stellar Astrophysics Centre (Aarhus) is provided by The Danish National Research Foundation. The research is supported by the ASTERISK project (ASTERoseismic Investigations with SONG and Kepler) funded by the European Research Council (Grant agreement no.: 267864). We thank the referee for helpful comments which helped to significantly improve the paper.

REFERENCES

- Alard, C., Lupton, R. H., 1998, *ApJ*, 503, 325
 Antoci V., et al., 2011, *Nature*, 477, 570
 Antoci, V., et al., 2013, in press, *MNRAS*
 Baker N., Kippenhahn R., 1962, *ZA*, 54, 114
 Baran A. S., Gilker J. T., Fox-Machado L., Reed M. D., Kawaler S. D., 2011, *MNRAS*, 411, 776
 Barclay T., Ramsay G., Hakala P., Napiwotzki R., Nelemans G., Potter S., Todd I., 2011, *MNRAS*, 413, 2696
 Bedding, T. R., et al., 2011, *Nature*, 471, 608
 Bertin E., Arnouts S., 1996, *A&AS*, 117, 393
 Breger, M., 2000, *ASP Con Series*, 210, 3
 Brown T. M., Latham D. W., Everett M. E., Esquerdo G. A., 2011, *AJ*, 142, 112
 Chaplin W. J., et al., 2011, *Sci*, 332, 213
 Devor, J., 2005, *ApJ*, 628, 411
 Dziembowski, W.; Krolikowska, M., 1990, *AcA*, 40, 19
 Eaton, N., Draper, P. W., & Allan, A., 2009, *Starlink User Note*, 45
 Feldmeier J. J., et al., 2011, *AJ*, 142, 2
 Graham, M. J., Drake, A. J., Djorgovski, S. G., Mahabal, A. A., Donalek, C., Duan, V., Maher, A., 2013, *MNRAS*, 434, 3423
 Greiss S., et al., 2012a, *AJ*, 144, 24
 Greiss S., et al., 2012b, *arXiv:1212.3613*
 Groot, P. J., et al., 2009, *MNRAS*, 399, 323
 Hambleton, K. M., et al, 2013, *MNRAS*, 434, 925
 Hartman J. D., Bakos G., Stanek K. Z., Noyes R. W., 2004, *AJ*, 128, 1761
 Hartman J. D., Gaudi B. S., Holman M. J., McLeod B. A., Stanek K. Z., Barranco J. A., Pinsonneault M. H., Kalirai J. S., 2008, *ApJ*, 675, 1254
 Hoffmeister, C., 1967, *AN*, 289, 205
 Howell, S. B., Everett, M. E., Seebode, S. A., Szkody, P., Still, M., Wood, M., Ramsay, G., Cannizzo, J., Smale, A., 2013, *AJ*, 145, 109
 Jeffery C. S., et al., 2013, *MNRAS*, 429, 3207
 Jester, S., et al, 2005, *AJ*, 130, 873
 Kato, T., Nogami, D., Baba, H., Masuda, S., 2001, *IBVS*, 5118
 Kinemuchi, K., Barclay, T., Fanelli, M., Pepper, J., Still, M., Howell, S. B., 2012, *PASP*, 124, 963
 Koch D. G., et al., 2010, *ApJ*, 713, L79
 Kurucz, R. L., 1992, *Rev Mex Astron Astro.*, 23, 181
 Lang D., Hogg D. W., Mierle K., Blanton M., Roweis S., 2010, *AJ*, 139, 1782
 Lemke, M. 1991, Internal Report, Department of Astronomy, University of Texas at Austin
 Lenz P., Pamyatnykh A. A., Zdravkov T., Breger M., 2010, *A&A*, 509, A90
 Lomb, N.R. 1976, *A&SS*, 39, 447
 McNamara, D. H., 1997, *PASP*, 109, 1221

- McNamara, D. H., 2000, Delta Scuti and Related Stars, Reference Handbook and Proc 6th Vienna Workshop in Astrophysics, ASPC, 210, 373
- Napiwotzki, R., et al, 2004, In *Spectroscopically and Spatially Resolving the Components of the Close Binary Stars*, ASP Conf Series, 318, 402
- Pamyatnykh, A. A., Delta Scuti and Related Stars, Reference Handbook and Proc 6th Vienna Workshop in Astrophysics, ASPC, 210, 215
- Patterson, J., et al. 2005, PASP, 117, 1204
- Pigulski A., Pojmański G., Pilecki B., Szczygiel D. M., 2009, AcA, 59, 33
- Pinsonneault M. H., An D., Molenda-Żakowicz J., Chaplin W. J., Metcalfe T. S., Bruntt H., 2012, ApJS, 199, 30
- Prša, A., et al., 2011, AJ, 141, 83
- Ramsay G., Hakala P., 2005, MNRAS, 360, 314
- Ramsay, G., Napiwotzki, R., Hakala, P., Lehto, H., 2006, MNRAS, 371, 957
- Ramsay, G., Napiwotzki, R., Barclay, T., Hakala, P., Potter, S., Cropper, M., 2011, MNRAS, 417, 400
- Ramsay, G., Doyle, J. G., Hakala, P., Garcia-Alvarez, D., Brooks, A., Barclay, T., Still, M., 2013, MNRAS, 434, 2451
- Scargle, J.D. 1982, ApJ, 263, 835
- Scaringi, S., Groot, P. J., Verbeek, K., Greiss, S., Knigge, C., Kolding, E., 2013, MNRAS, 428, 2207
- Schwarzenberg-Czerny A., 1989, MNRAS, 241, 153
- Schwarzenberg-Czerny A., 1996, ApJ, 460, L107
- Shibahashi, H., Kurtz, D. W., 2012, MNRAS, 422, 738
- Slawson, R. W., et al, 2011, AJ, 142, 160
- Southworth, J., et al, 2011, MNRAS, 414, 2413
- Tamuz O., Mazeh T., Zucker S., 2005, MNRAS, 356, 1466
- Tamuz O., Mazeh T., North P., 2006, MNRAS, 367, 1521
- Thompson, S. E., et al., 2012, ApJ, 753, 86
- Uytterhoeven K., et al., 2011, A&A, 534, A125
- Warner, B. 1995, Cataclysmic Variable Stars (Cambridge: Cambridge)
- Welsh W. F., et al., 2011, ApJS, 197, 4
- Wozniak P. R., 2000, AcA, 50, 421

APPENDIX A: TABLES

Table A1. List of fields observed using in the INT in 2011, field ID corresponds to our own internal designations, field centres correspond to a point in CCD 4.

Date (dd-mm-yy)	Field ID	RA DEC (J2000)	Date(dd-mm-yy) (dd-mm-yy)	Field ID	RA DEC (J2000) (J2000)
11-07-11	522	19:46:51 +49:43:35	02-08-11	382	19:22:42 +50:39:03
11-07-11	542	19:45:05 +47:36:21	02-08-11	408	19:23:33 +49:11:06
11-07-11	541	19:46:43 +47:14:21	03-08-11	46	19:01:23 +40:59:18
11-07-11	349	19:39:18 +39:16:51	03-08-11	63	19:05:58 +37:58:36
11-07-11	539	19:49:56 +46:30:21	03-08-11	260	19:11:38 +46:19:02
11-07-11	567	19:57:19 +43:59:07	03-08-11	73	19:11:46 +38:20:36
11-07-11	570	19:52:40 +45:05:09	03-08-11	259	19:13:14 +45:57:02
12-07-11	94	18:44:31 +47:36:58	03-08-11	380	19:14:02 +51:34:03
12-07-11	100	18:45:45 +48:09:58	03-08-11	373	19:14:10 +50:39:03
12-07-11	93	18:46:25 +47:14:58	04-08-11	72	19:02:36 +39:37:36
12-07-11	234	18:57:27 +49:21:54	04-08-11	236	19:06:53 +48:26:54
12-07-11	575	19:55:42 +45:16:09	04-08-11	264	19:16:22 +46:08:02
12-07-11	503	19:53:20 +42:09:20	04-08-11	296	19:18:56 +45:13:52
12-07-11	488	19:53:27 +40:19:20	04-08-11	277	19:19:29 +47:14:02
13-07-11	99	18:47:40 +47:47:58	04-08-11	269	19:19:33 +46:19:02
13-07-11	105	18:48:54 +48:20:58	04-08-11	406	19:26:55 +48:27:05
13-07-11	92	18:48:18 +46:52:58	05-08-11	245	19:02:50 +50:05:54
13-07-11	157	19:15:34 +42:19:19	05-08-11	76	19:07:31 +39:26:36
13-07-11	469	19:43:31 +44:27:24	05-08-11	281	19:20:36 +43:01:58
13-07-11	446	19:40:23 +46:44:30	05-08-11	223	19:28:21 +39:15:28
13-07-11	354	19:42:06 +39:27:51	05-08-11	325	19:36:07 +41:32:30
14-07-11	104	18:50:50 +47:58:58	05-08-11	583	20:06:28 +44:32:07
14-07-11	97	18:51:29 +47:03:58	05-08-11	585	20:03:23 +45:16:09
14-07-11	103	18:52:45 +47:36:58	06-08-11	578	20:01:52 +44:43:09
14-07-11	110	18:54:01 +48:09:58	06-08-11	555	19:59:31 +47:03:21
14-07-11	204	19:24:20 +37:36:28	06-08-11	499	19:59:13 +40:41:20
14-07-11	214	19:29:50 +37:58:28	06-08-11	566	19:58:51 +43:37:09
14-07-11	213	19:31:14 +37:36:28	06-08-11	580	19:58:44 +45:27:07
15-07-11	8	18:46:20 +42:51:19	06-08-11	588	19:58:37 +46:22:09
15-07-11	7	18:48:05 +42:29:19	06-08-11	556	19:57:53 +47:25:21
15-07-11	12	18:51:04 +42:40:19	07-08-11	581	19:57:09 +45:49:09
15-07-11	18	18:52:17 +43:13:19	07-08-11	494	19:54:53 +40:52:20
15-07-11	321	19:31:44 +41:43:30	07-08-11	550	19:54:41 +47:14:21
15-07-11	297	19:28:09 +43:56:55	07-08-11	562	19:54:17 +43:48:09
15-07-11	328	19:31:40 +42:38:30	07-08-11	559	19:52:56 +48:31:21
16-07-11	114	18:57:18 +44:04:28	07-08-11	563	19:52:45 +44:10:09
16-07-11	120	18:58:32 +44:37:28	07-08-11	471	19:52:37 +43:10:24
16-07-11	126	18:59:46 +45:10:28	08-08-11	538	19:51:32 +46:08:21
16-07-11	314	19:31:45 +40:48:30	08-08-11	560	19:51:16 +48:53:21
16-07-11	309	19:28:51 +40:37:30	08-08-11	483	19:50:35 +40:08:20
16-07-11	338	19:35:06 +38:32:48	08-08-11	490	19:50:33 +41:03:20
16-07-11	219	19:34:00 +37:47:28	08-08-11	497	19:50:28 +41:58:18
17-07-11	28	18:48:05 +44:52:19	08-08-11	528	19:50:12 +49:54:35
17-07-11	27	18:49:54 +44:30:19	08-08-11	465	19:49:37 +42:59:24
17-07-11	133	18:59:24 +46:05:28	09-08-11	473	19:49:34 +43:54:24
17-07-11	55	18:59:05 +42:16:18	09-08-11	477	19:49:10 +39:35:20
17-07-11	412	19:28:28 +49:00:06	09-08-11	484	19:49:09 +40:30:20
17-07-11	436	19:32:35 +46:44:27	09-08-11	521	19:48:33 +49:21:35
17-07-11	439	19:38:53 +46:11:30	09-08-11	533	19:48:22 +45:57:19
01-08-11	36	18:55:39 +40:37:18	09-08-11	540	19:48:20 +46:52:21
01-08-11	238	19:02:58 +49:10:54	09-08-11	466	19:48:07 +43:21:23
01-08-11	139	19:02:58 +46:16:28	10-08-11	530	19:46:45 +50:38:35
01-08-11	131	19:03:05 +45:21:28	10-08-11	548	19:46:36 +48:09:21
01-08-11	376	19:21:01 +50:06:03	10-08-11	467	19:46:35 +43:43:23
02-08-11	240	18:59:00 +49:54:54	10-08-11	486	19:46:14 +41:14:17
02-08-11	151	19:03:09 +43:25:19	10-08-11	516	19:45:13 +49:10:35
02-08-11	141	19:08:12 +41:24:19	10-08-11	535	19:45:11 +46:41:21
02-08-11	154	19:09:37 +42:52:19	10-08-11	454	19:45:09 +42:15:24
02-08-11	390	19:22:35 +51:34:03			

Table A2. List of fields observed using in the INT in 2012, field ID corresponds to our own internal designations, field centres correspond to a point in CCD 4.

Date (dd-mm-yy)	Field ID	RA DEC (J2000)	Date (dd-mm-yy)	Field ID	RA DEC (J2000) (J2000)
03-08-12	5	18:39:52 +43:24:19	08-08-12	1010	19:20:19 +43:38:30
03-08-12	67	18:59:22 +39:26:36	08-08-12	203	19:25:43 +37:14:28
03-08-12	144	19:03:15 +42:30:19	08-08-12	251	19:06:41 +50:16:54
03-08-12	300	19:23:31 +45:02:56	08-08-12	289	19:19:02 +44:18:58
05-08-12	463	19:42:05 +43:54:24	08-08-12	383	19:20:57 +51:01:03
05-08-12	1001	18:45:00 +47:21:36	09-08-12	1005	19:12:34 +43:30:14
05-08-12	1007	18:59:02 +48:42:37	09-08-12	1006	19:17:19 +39:27:18
05-08-12	155	19:08:06 +43:14:17	10-08-12	1006	19:17:19 +39:27:18
05-08-12	568	19:55:46 +44:21:07	10-08-12	1008	19:11:33 +45:43:44
05-08-12	463	19:42:05 +43:54:24	10-08-12	210	19:25:41 +38:09:28
05-08-12	546	19:49:53 +47:25:22	10-08-12	222	19:29:47 +38:53:28
05-08-12	523	19:45:08 +50:05:35	10-08-12	365	19:15:57 +49:22:03
06-08-12	1	18:46:52 +41:56:18	10-08-12	368	19:10:48 +50:28:03
06-08-12	1002	19:04:62 +42:45:48	10-08-12	374	19:12:25 +51:01:03
06-08-12	168	19:10:56 +44:20:19	11-08-12	1009	19:09:59 +47:17:07
06-08-12	175	19:17:49 +39:37:14	11-08-12	1011	19:18:30 +45:33:11
06-08-12	181	19:19:14 +40:10:15	11-08-12	1012	19:19:12 +49:57:51
06-08-12	305	19:28:07 +44:52:02	11-08-12	292	19:25:07 +43:45:58
06-08-12	342	19:39:19 +38:21:51	11-08-12	359	19:46:21 +39:16:51
07-08-12	1013	19:29:12 +50:19:02	11-08-12	392	19:19:00 +52:18:03
07-08-12	226	19:00:03 +48:04:54	11-08-12	401	19:23:41 +48:16:06
07-08-12	239	19:00:59 +49:32:54	12-08-12	10	18:42:48 +43:35:20
07-08-12	311	19:25:55 +41:21:30	12-08-12	2	18:45:08 +42:18:20
07-08-12	327	19:33:09 +42:16:30	12-08-12	3	18:43:23 +42:40:20
07-08-12	332	19:37:34 +42:05:30	12-08-12	4	18:41:38 +43:02:20
07-08-12	351	19:36:26 +40:00:51	12-08-12	496	19:51:57 +41:36:20
08-08-12	1003	19:06:31 +43:54:48	12-08-12	6	18:49:50 +42:07:20
08-08-12	1004	19:19:55 +42:47:29	12-08-12	9	18:44:35 +43:13:20

Table A3. List of fields observed using the MDM 1.3m telescope in 2012, field ID corresponds to our own internal designations, field centres correspond to a point approximately in the centre of the chip.

Date (dd-mm-yy)	Field ID	RA DEC (J2000)	Date (dd-mm-yy)	Field ID	RA DEC (J2000)
16-05-2012	81	19:12:07 +39:16:50	21-05-2012	174	19:19:15 +39:15:15
16-05-2012	82	19:10:42 +39:38:50	21-05-2012	175	19:17:49 +39:37:15
16-05-2012	83	19:09:16 +40:00:51	21-05-2012	226	19:00:03 +48:04:55
16-05-2012	84	19:07:49 +40:22:55	21-05-2012	351	19:36:26 +40:00:51
17-05-2012	85	18:49:13 +45:58:48	22-05-2012	212	19:22:51 +38:53:28
19-05-2012	135	19:10:10 +44:50:04	22-05-2012	218	19:24:11 +39:26:28
19-05-2012	142	19:07:08 +41:47:26	22-05-2012	273	19:13:03 +47:47:02
19-05-2012	149	19:07:04 +42:42:34	22-05-2012	95	18:42:35 +47:58:58
19-05-2012	89	18:41:41 +47:26:48	23-05-2012	106	18:46:58 +48:42:58
20-05-2012	122	18:54:54 +45:21:28	23-05-2012	286	19:23:37 +43:12:58
20-05-2012	160	19:11:03 +43:25:19	23-05-2012	288	19:20:34 +43:56:58
20-05-2012	161	19:09:32 +43:47:19	23-05-2012	329	19:30:09 +43:00:30
20-05-2012	162	19:08:00 +44:09:19			

Table A4. The full set of parameters which are included in our data products.

Parameter	Notes
KIC_ID	The <i>Kepler</i> Input Catalog (Brown et al. 2011) star number;
RA, DEC	Right Ascension and Declination (J2000);
g_{mag}	Taken from the KIS, Greiss et al. (2012a,b);
g_{err}	Taken from the KIS Greiss et al. (2012a,b);
U_g, g_r	$(U - g)$, $(g - r)$ taken from Greiss et al. (2012a,b);
LS_Period	The period of the most prominent peak in the Lomb Scargle periodogram in days and LS_Period_Mins (mins);
Log10_LS_Prob	The False Alarm Probability of the most prominent period in the Lomb Scargle periodogram (in units of log 10);
Alarm	The alarm variability statistic (Tamuz, Mazeh, and North 2006);
AoV_Period	The Period determined from the AoV test in days and AOV_Period_Mins (mins);
AoV	The AoV variability statistic Schwarzenberg-Czerny (1989, 1996);
AOV_SNR	the S/N ratio of the peak measured over the full periodogram;
AOV_NEG_LN_FAP	The negative of the natural logarithm of the formal false alarm probability;
Chi2	The reduced χ^2 value of the light curve tested against the constant mean value (with 5σ clipping);
StdDev	the standard deviation (root mean squared) of the light curve;
Field	Our internal naming convention for the field pointing;
Chip	For the INT/WFC the chip id. There was only one chip for the MDM observations;
FieldChip	The Field-Chip Combination
ID	Our internal naming convention for the source. A 6 digit number implies the light curve was derived; using <code>diapl</code> , while for those derived using <code>sextractor</code> , the numbering system starts from 1;
X, Y	The X, Y coordinates of the source on the chip;
grats, g_r_rats	The g mag and $(g - r)$ colour at the time of our observations;
Flag	'0' Variability on <code>ls_per_min</code> ; '1' Probable variability on <code>ls_per_min</code> ; '2' Clear long timescale high amplitude variable; '3' Not variable on <code>ls_per_min</code> ; '4' Variable on period other than <code>ls_per_min</code> ; '5' Possible variability in general; '6' not likely to be variable; '7' bad light curve; '8' Eclipse; '9' Possible eclipse; '10' Variability likely due to systematic trend; '11' Known bad columns on chip; '12' Apparent long period could be due to residual systematic trends; '13' Image shows close stellar companion;
Tstart, Tstop	The start and end date in MJD of the sequence of g band observations.
medFAP	The median log FAP for the chip which the source is located

Table A5. Table showing all of our variable stars selected using 'n=18' and which passed our manual verification phase (see §3.2) along with a selection of parameters.

KIC ID	RA J2000	DEC J2000	g_{KIS} mag	$(U - g)_{KIS}$ mag	$(g - r)_{KIS}$ mag	g_{rats} mag	$(g - r)_{rats}$ mag	Alarm	AOV Period mins	AOV	LS_Per mins	LS_Log_FAP
11911480	19:20:24.91	+50:17:22.4	18.09	-0.39	0.06	18.13	-0.05	0.02	4.89	14.75	4.9	-6.93
8293193	19:17:55.25	+44:13:26.1	18.42	-0.31	0.08	18.41	0.00	1.88	5.17	5.81	5.2	-4.46
	19:29:00.80	+44:56:59.2				13.95		1.43	9.93	9.29	10.1	-5.51
12647528	19:22:50.90	+51:45:31.5	14.31	1.73	1.05	14.35	0.99	2.75	43.4	10.36	10.8	-4.83
10728590	19:23:18.49	+48:02:09.0	19.14		0.97	19.37	1.01	4.25	13.9	8.73	13.8	-4.81
10936077	19:52:53.44	+48:19:35.6	15.85	0.70	0.70	15.90	0.56	2.62	31.8	12.19	16.2	-4.80
7356523	19:19:30.70	+42:58:08.5	19.20	0.94	0.65	19.20	0.65	2.00	18.8	6.91	18.5	-4.44
9899481	19:41:00.84	+46:44:58.3	19.66	0.49	0.64	19.61	0.53	2.99	36.4	10.77	19.3	-5.11
6665002	18:46:27.78	+42:10:34.9	19.50	0.13	0.68	19.45	0.64	3.34	21.0	9.38	21.2	-4.66
8123702	19:57:39.81	+43:55:07.7	13.46	2.04	1.17	13.50	1.11	4.54	64.9	8.78	21.8	-3.98
	18:55:13.43	+43:57:31.6	19.75			19.61	1.08	2.21	22.9	8.10	23.2	-3.83
6109859	19:07:56.19	+41:26:33.1	16.19	0.35	0.17	16.19	0.17	8.22	23.1	39.38	23.4	-11.64
3223460	19:12:32.15	+38:23:00.1	13.71	0.27	0.25	13.74	0.16	7.58	24.4	29.58	24.0	-10.71
	19:53:11.03	+48:39:39.1				14.79	0.63	4.06	44.6	14.76	25.9	-5.42
	19:18:03.08	+39:26:21.8						5.28	26.4	16.88	26.2	-8.03
11360026	19:45:03.62	+49:06:01.0	15.01	0.24	0.29	14.99	0.16	9.25	32.9	18.47	32.5	-9.59
9813390	18:49:08.86	+46:40:04.2	16.86	1.30	1.14	16.98	1.04	10.29	66.2	24.35	34.7	-5.17
10031075	19:54:21.16	+46:57:39.9	15.17	0.63	0.76	15.18	0.64	2.71	38.2	9.62	35.1	-5.57
8118210	19:52:18.66	+43:58:11.8	17.02	0.46	0.47	17.09	0.33	3.98	65.4	12.07	35.4	-6.31
7960631	19:28:05.53	+43:45:45.5	15.31	0.30	0.31	15.32	0.18	7.28	63.5	23.15	35.6	-7.96
9479634	19:48:39.16	+46:03:47.1	14.65	0.39	0.32	14.63	0.20	11.23	36.0	51.00	36.4	-12.4
5772488	19:00:07.98	+41:02:51.8	17.67	0.21	0.33	17.70	0.16	9.54	65.5	22.88	37.3	-8.15
11723564	19:47:11.37	+49:53:13.7	12.81	0.38	0.40	12.74	0.17	7.47	66.4	18.83	38.0	-7.91
10253681	18:46:40.86	+47:18:28.1	17.22	0.60	0.69	17.04	0.63	5.61	37.6	25.38	39.6	-8.51
9786930	19:51:01.55	+46:34:24.6	19.00	1.29	1.00	19.03	0.77	8.33	47.3	18.77	41.1	-6.77
10975348	19:26:46.09	+48:25:30.9	18.88	0.19	0.34	18.72	0.07	13.32	54.0	32.84	41.2	-9.59
9364179	19:56:24.52	+45:48:24.1	14.38	0.44	0.43	14.42	0.36	6.93	43.4	17.11	41.2	-7.51
9294308	19:47:09.39	+45:44:32.1	13.66	0.25	0.34	13.64	0.19	6.09	44.7	17.89	42.9	-8.05
7698266	19:46:50.79	+43:19:02.3	13.22	0.21	0.41	13.26	0.32	6.54	43.7	18.00	43.6	-7.86
10353926	19:47:53.67	+47:26:56.3	14.89	0.22	0.28	14.90	0.31	9.32	45.0	26.15	44.1	-9.90
7625723	19:47:11.80	+43:16:37.4	14.18	1.42	1.02	14.21	0.95	8.22	48.7	19.43	44.2	-7.70
9417741	19:47:39.58	+45:55:07.6	14.72	0.29	0.28	14.78	0.20	15.78	45.3	75.25	44.4	-13.3

Table A5. Table showing all of our variable stars selected using ' $n=18$ ' and which passed our manual verification phase (see §3.2) along with a selection of parameters.

KIC ID	RA J2000	DEC J2000	g_{KIS} mag	$(U-g)_{KIS}$ mag	$(g-r)_{KIS}$ mag	g_{rats} mag	$(g-r)_{rats}$ mag	Alarm	AOV	Period mins	AOV	LS_Per mins	LS_Log_FAP
4262791	19:26:48.06	+39:20:35.7	15.74	4.82	0.26	15.71	0.21	13.49		62.9	23.15	44.5	-7.60
12406812	19:23:33.80	+51:17:58.9	17.24	0.17	0.36	17.24	0.21	14.47		46.8	47.66	46.5	-12.06
7548311	19:48:28.48	+43:06:12.3	14.55	0.47	0.48	14.52	0.34	10.56		66.5	32.02	46.7	-9.56
5623923	19:32:01.53	+40:51:16.8	16.61	0.23	0.27	16.57	0.15	10.30		45.3	23.26	47.4	-10.24
6418095	18:44:56.53	+41:50:28.1	13.20	0.12	0.23	13.14	0.23	10.41		47.4	35.16	48.3	-11.61
7770746	19:49:00.55	+43:26:06.4	18.84	1.41	1.16	19.20	1.35	17.02		47.6	72.20	48.5	-13.46
9640005	19:09:46.28	+46:20:04.1	18.39	0.15	0.21	18.39	0.15	18.18		63.9	50.71	48.5	-11.27
9786165	19:50:10.98	+46:34:40.8	17.66	0.81	0.76	18.39	1.12	16.50		47.3	47.53	49.7	-10.19
5474065	19:53:02.53	+40:40:34.6	18.77	1.93	1.43	18.76	1.39	12.75		51.3	105.44	49.9	-6.32
9672731	19:59:30.69	+46:23:06.7	17.47	0.97	0.98	17.95	1.16	8.185		66.2	18.77	51.1	-8.65
8840638	19:55:35.07	+45:04:46.0	14.63	0.52	0.54	14.71	0.42	22.33		49.8	98.99	51.6	-14.54
9720306	19:43:03.19	+46:25:56.0	15.45	0.28	0.33	15.50	0.23	15.80		49.7	30.96	51.9	-10.27
6029053	19:08:02.00	+41:22:12.6	17.51	3.21	1.43	17.51	1.43	13.82		55.1	76.53	52.9	-7.61
8117771	19:51:52.82	+43:55:00.1	13.24	0.26	0.36	13.22	0.25	17.99		54.2	59.45	53.4	-12.18
8387281	19:54:08.13	+44:22:16.5	15.65	1.65	1.47	15.64	1.46	7.73		45.5	49.45	55.6	-6.74
4389023	19:47:47.78	+39:29:41.5	13.63	0.21	0.36	13.64	0.25	18.31		52.3	59.75	56.8	-12.35
5818101	19:54:18.14	+41:04:07.1	17.52	0.25	0.39	17.48	0.28	17.61		65.1	32.50	57.4	-11.32
7839261	19:48:18.90	+43:34:22.1	14.77	0.39	0.40	14.77	0.31	22.00		57.2	92.79	58.0	-13.31
8118471	19:52:35.03	+43:56:42.3	15.72	0.45	0.56	15.75	0.46	12.94		60.8	28.50	59.2	-10.42
5179693	19:18:32.80	+40:22:51.3	17.60	0.17	0.32	17.74	0.29	19.35		65.8	64.82	61.3	-12.62
7768746	19:47:00.08	+43:28:22.2	13.23	0.38	0.58	13.18		18.11		54.1	78.36	61.5	-12.69
3350736	19:34:23.34	+38:24:30.5	15.47	0.30	0.45	15.53	0.33	23.04		64.3	41.69	62.1	-11.50
10284901	19:43:46.41	+47:20:32.8	15.72	0.06	0.31	15.59	0.11	19.40		64.4	161.97	62.1	-13.80
8255272	19:53:55.44	+44:11:49.4	13.24	0.28	0.41	13.18	0.44	17.86		62.1	49.52	63.0	-11.85
9364721	19:57:04.39	+45:48:41.1	19.06	0.60	0.85	19.06	0.71	10.03		64.2	19.32	63.7	-8.99
8908767	19:56:07.19	+45:08:50.8	14.30	0.56	0.55	14.35	0.46	21.59		66.4	118.8	64.0	-14.48
9905251	19:48:41.25	+46:43:33.9	16.11	0.30	0.35	16.13	0.18	17.04		55.9	40.88	64.4	-12.30
9812716	18:47:14.89	+46:36:38.4	13.95	0.28	0.29	13.91	0.14	13.67		52.7	38.82	64.9	-11.91
	19:16:43.60	+39:31:27.8						17.24		62.2	61.85	65.2	-12.21
8254486	19:53:11.74	+44:07:43.2	14.76	0.42	0.58	14.59	0.48	17.17		56.6	47.02	65.2	-12.13
4916020	19:17:58.54	+40:04:54.6	14.57	0.33	0.31	14.53	0.28	13.69		61.9	47.96	65.8	-11.79
4149801	19:18:07.97	+39:15:42.0	19.51	1.56	1.21	19.74	2.04	18.62		54.2	58.62	66.1	-11.72
8561192	19:29:05.17	+44:41:50.8	16.43	0.34	0.49	16.40	0.48	17.05		66.5	62.97	66.5	-10.86